

Synthesis and characterization of SnO₂ Nanoparticles for PV Applications

*Saira Riaz¹⁾, Adeela Nairan²⁾ and Shahzad Naseem¹⁾

¹⁾ Centre of Excellence in Solid State Physics, University of the Punjab, Pakistan

²⁾ Centre for High Energy Physics

¹⁾ shahzad_naseem@yahoo.com

ABSTRACT

Tin oxide nanoparticles have been prepared by conventional sol-gel technique. Research grade tin chloride (SnCl₂·2H₂O) was used as tin and zinc sources. Ethylene glycol and alcohol were used as solvents under different synthesis conditions. Transparent un-doped SnO₂ sol was prepared after continuous stirring and refluxing at 40°C. Thin films, prepared from SnO₂ sol, have also been deposited on glass substrate by spin coating at 500 rpm for 10 seconds and then at 3000rpm for 30 seconds. Scanning electron microscopy results show the formation of nanodiamonds (~40 nm) and nanorods (~30 nm) after annealing at 300°C for 60 minutes. It is important to mention here that we have prepared SnO₂ nanostructures without the use of any surfactant and ligand during sol synthesis. X-ray diffraction (XRD) patterns show that the preferred orientation was (111) with orthorhombic crystal structure. Crystallite size was calculated to be ~8 nm from XRD results. Optical properties measured by using spectroscopic ellipsometer have shown a band gap of 3.87 eV, which is larger than the band gap of SnO₂ in bulk form (3.6 eV). More than 90% transmission was observed in these sol-gel deposited SnO₂ thin films

1. INTRODUCTION

Due to their unique electronic, optical and mechanical properties (Zheng 2001) one dimension (1D) nanoscale materials have gained many scientist's attention. At this structural level, nanosized semi-conducting oxide materials show the properties such as super-conductivity, ferro-electricity and magnetism etc. covering all the aspects of material science.

Conductive oxides are promising materials for the manufacture of transparent electronics and optoelectronic devices in the ultraviolet (UV) region due to their wide band gap and high mobility.

The control of sizes and shapes of nanostructures is crucial as it may affect their electrical and optical properties (Lim 2011, Baruah 2009). For controlling the size of particles we have used sol-gel method. There are many advantages of sol-gel method

¹⁾ Professor

²⁾ Graduate Student

such as it allows the production of new hybrid organic-inorganic materials, which do not exist in nature. Furthermore, it is cost-effective and large-area scalable technique.

In this paper, we report on the sol-gel prepared un-doped and ZnO doped SnO₂. Stannous chloride hydrate (SnCl₂.2H₂O) was used as a precursor. The structural and morphological characterization was carried out by XRD, SEM and AFM. Effect of doping and synthesis parameters on the optical properties were also studied.

2. EXPERIMENTAL DETAILS

2.1 Synthesis of SnO₂ Sol

In this technique tin chloride hydrate SnCl₂.2H₂O was used as starting material. A solution of 0.1 mol % SnCl₂ in ethylene glycol was prepared by dissolving appropriate amounts of SnCl₂ under vigorous stirring at 60°C until colorless and transparent sol was obtained. Before gelation process thin films were also prepared on glass substrate by spin coating. Samples were dried at room temperature for 24h and then annealed at 300°C for 1h.

2.2 Characterization

Crystallographic structure along with the phase variation and crystallite size of undoped and doped SnO₂ samples was studied by Rigaku D-MAX/IIA X-ray diffractometer (XRD). CuK α (Ni filtered) radiations ($\lambda=1.5405$ Å) were used to obtain the XRD pattern. Surface morphology was observed using Hitachi S-3400N scanning electron microscope (SEM). Bruker CP-II atomic force microscopy (AFM) was used to characterize the surface nanostructure. Optical properties in the UV-VIS-IR range were obtained by using JA Woollam's variable angle spectroscopic ellipsometer (VASE).

3. RESULTS AND DISCUSSION

Fig. 1 shows XRD pattern of SnO₂ nanoparticles under as-synthesized and annealed conditions of 200°C-500°C. All the peaks are well consistent with JCPDS card no. (29-1484), which confirmed the samples as pure orthorhombic crystalline SnO₂.

XRD plot of as synthesized samples confirm the crystalline structure of SnO₂ without any heat treatment. To obtain more quantitative information, the XRD pattern was analyzed with Gaussian function where full widths at half maxima [FWHM] were determined. The grain size of SnO₂ thin film (D) can be estimated by the Debye-Scherrer formula in Eq. (1) and shown in Fig. 2.

$$D = \frac{0.9\lambda}{B \cos \theta} \quad (1)$$

Where, D = Crystalline grain size, B = FWHM of the diffracted peak, λ = wavelength of the X-rays, θ = Angle of diffraction.

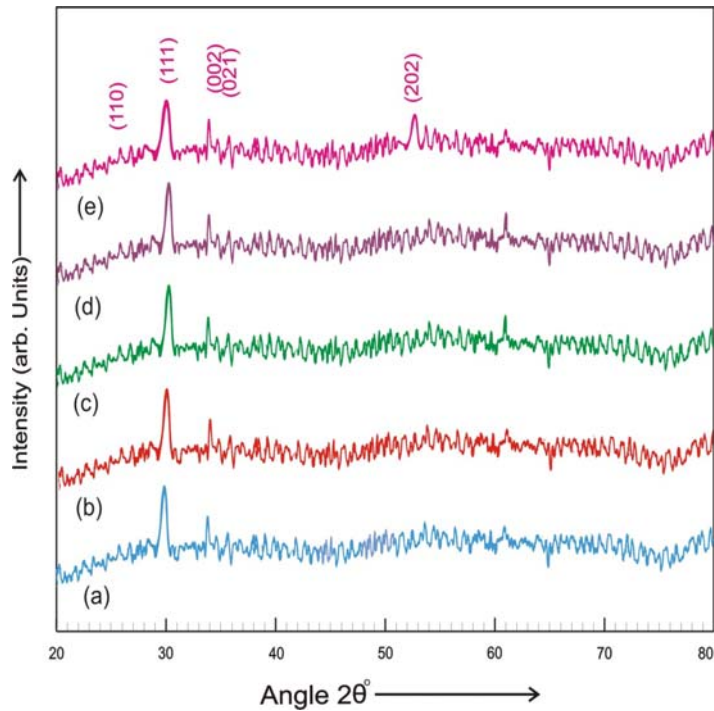


Fig. 1 XRD pattern of SnO₂ nanoparticles (a) as-synthesized; (b) 200°C; (c) 300°C; (d) 400°C; and (e) 500°C

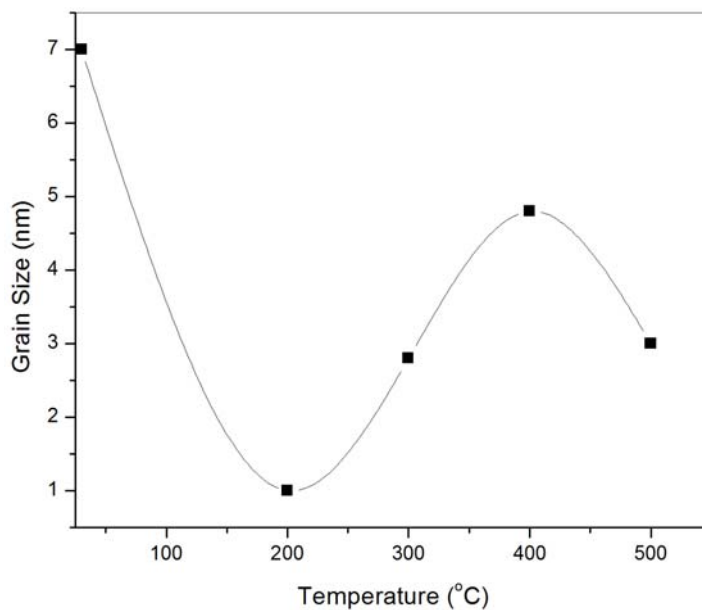


Fig. 2 Variation in Crystallite size with temperature

Using Scherrer formula in Eq. (1) the average crystallite size is calculated to be 2.4 nm, 3.9 nm, 5.6 nm, 6 nm, 4 nm.

In the polycrystalline structures, generally the major structure or orientation mainly depends on the processing parameters. During the coalescence of two differently

oriented nuclei the structural changes occur by surface diffusion and migration of grain boundaries. In such cases, smaller nuclei may easily rotate on coalescence that causes the structural changes. The lowest surface energy, the grain boundary energy and the diffusion of surface atoms influence the stable polycrystalline state of a material.

The reports by Lee (2008) reveal that the preferred orientation of grain growth and the final texture of thin films depend on the strain energy minimization and surface energy minimization. The level of these energy states depends on the thickness of the films. The minimization of strain energy supports one type of texture while the minimization of surface energy promotes another. Furthermore, surface energy dominates at a lower surface to volume ratio, whereas at the higherratio strain energy will be significant.

In XRD patterns, shown in Fig. 1, peak broadening is observed with increase in annealing temperature. The relationship between the broadening produced and stress/strain can be found by differentiating the Bragg's law as given in Eq. (2) (Cullity 1978).

$$b = \Delta 2\theta = -2 \frac{\Delta d}{d} \tan \theta \quad (2)$$

Where, b = extra broadening and $\Delta d/d$ = variation in strain.

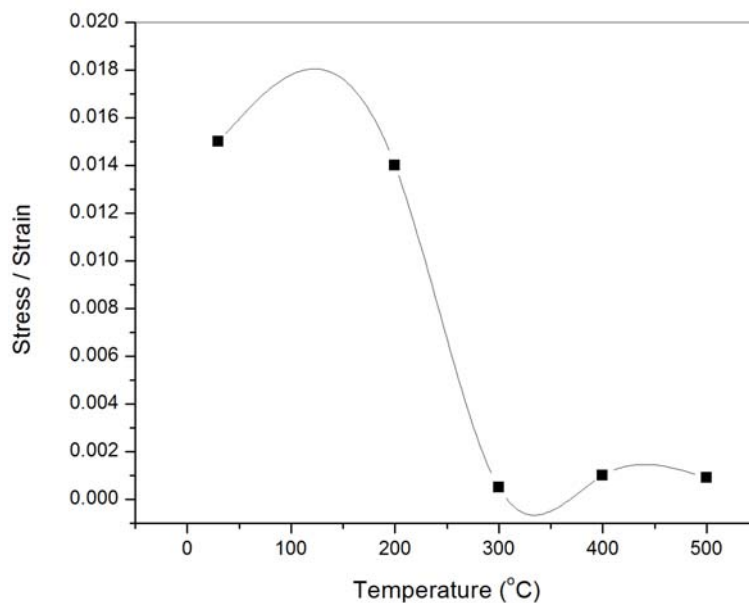
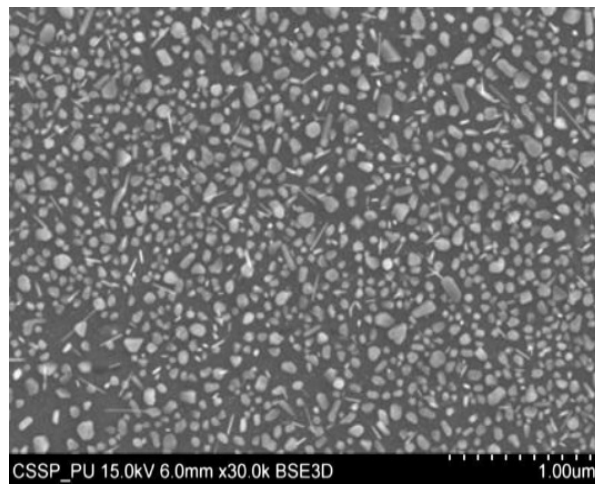
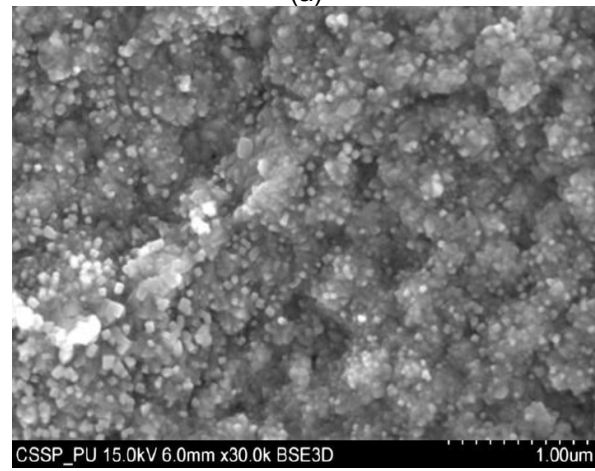


Fig. 3 Variation in Stress / Strain of SnO₂ samples

Fig. 4 shows SEM micrographs of SnO₂ nanostructures. Free large-area growth of nanorods and nanodiamonds of diameter 30 nm and 40 nm respectively, was observed. Pal (2009) reported SnO₂ nanostructures with use of cationic surfactant but it is worth mentioning here that these nanostructures are formed without the use of any surfactant during sol synthesis.

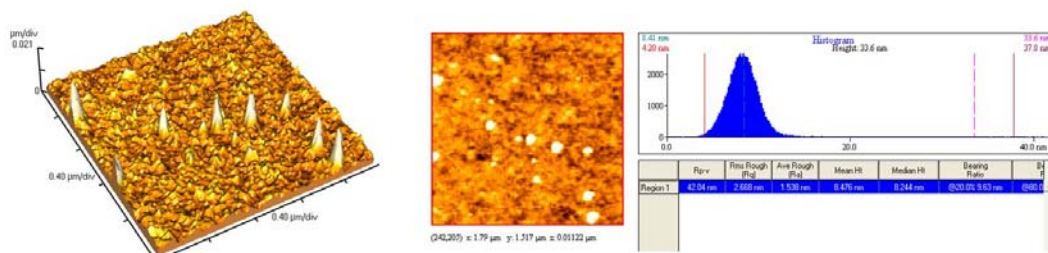


(a)

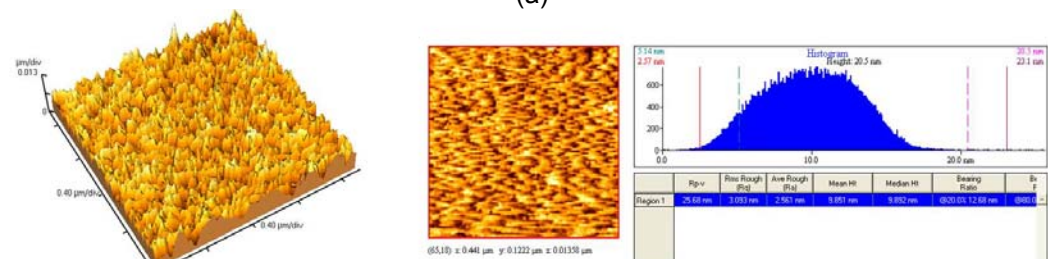


(b)

Fig. 4 SEM micrographs of SnO₂ nanostructures at (a) 200°C and (b) 300°C



(a)



(b)

Fig. 5 AFM images of SnO₂ nanostructures at (a) 200°C and (b) 300°C

Fig. 5 shows surface morphologies of SnO₂ nanostructures annealed at 200°C and 300°C. It can be seen that films are extremely smooth with RMS surface roughness of less than 3nm.

Thin films of SnO₂ nanostructures were prepared by spin coating to observed the optical properties. The transmittances of SnO₂ films with different annealing conditions are shown in Fig. 6. The average transmittance of thin films at 339 nm is above 85% for all films, which is in good agreement with the reported values (Shamala 2004). Generally the required transmittance of transparent conductive thin film for solar cells is

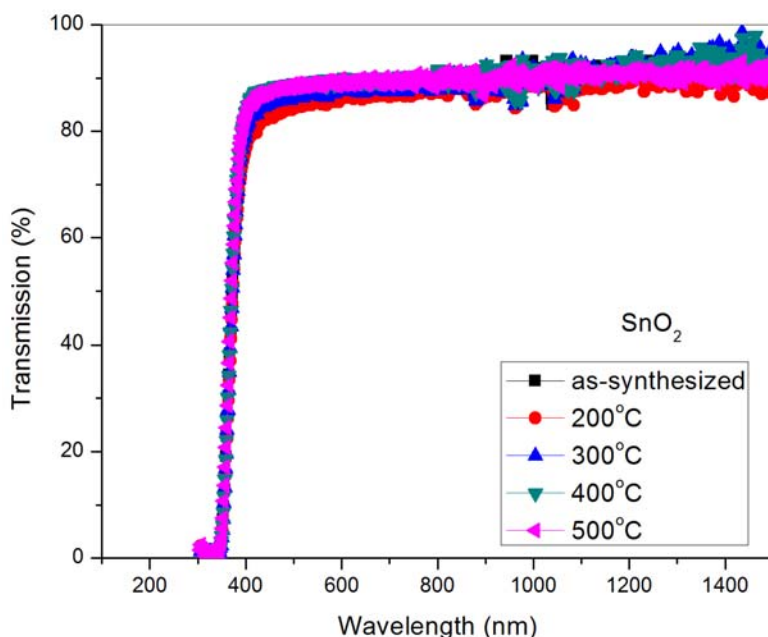


Fig. 6 Transmission spectra of SnO₂ Films prepared by using nanostructures

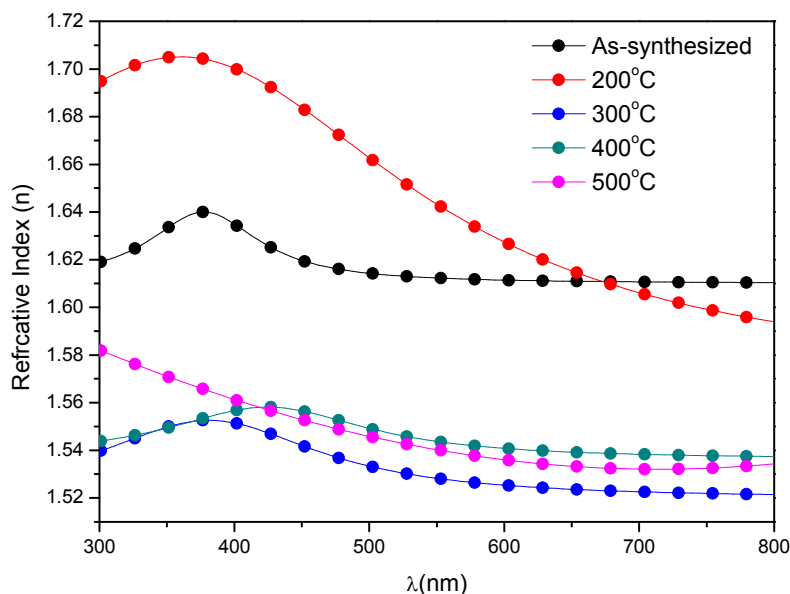


Fig. 7 Variation in refractive index 'n' of SnO₂ Thin films prepared by using nanoparticles

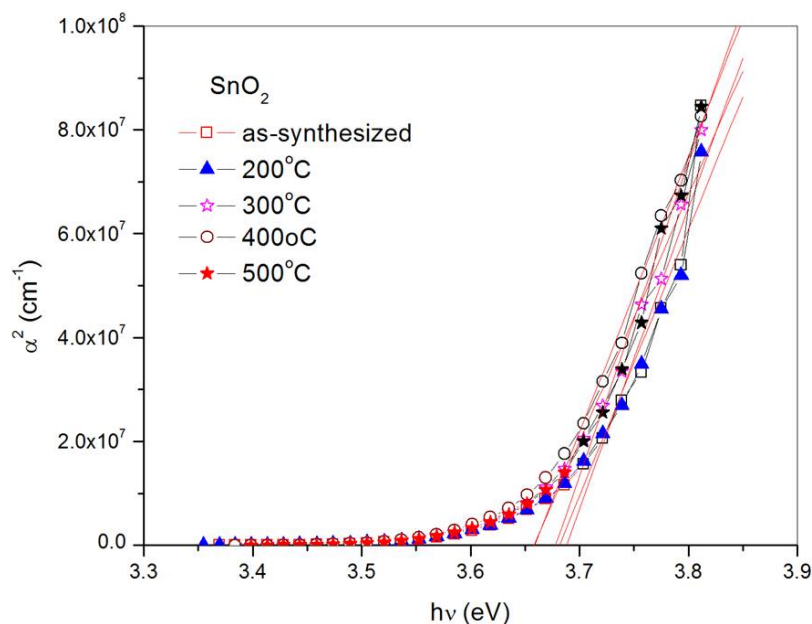


Fig. 8 Band gap variation of SnO₂ Thin films prepared by using nanoparticles

over 85% and as such these results indicate that SnO₂ thin films are a good candidate to be used as a window layer in solar cells.

Fig. 7 shows refractive indices values for SnO₂. The peak of refractive index at ~350 nm corresponds to direct band gap transition. Variations in refractive index are observed with changes in temperatures. For SnO₂ thin films the refractive index increases upto a temperature of 300°C after which the refractive index decreases. Refractive indices are in the range of 1.55-1.75.

The direct band gap is extracted by linear extrapolation of α^2 vs. E (eV) plot to zero on the energy axis. Fig. 8 shows the band gap of SnO₂ Thin films prepared by using nanoparticles. Band gap lies in the range of 3.66-3.68eV our results are in good agreement with those reported in literature.

3. CONCLUSIONS

Tin oxide (SnO₂) nanostructures are prepared via cost effective and application oriented sol-gel route. Nanoparticles are annealed up to 500°C. XRD results confirmed the orthorhombic crystalline structure of SnO₂ nanoparticles. SEM images show the formation of nanorod (30nm) and nanodiamond (40nm). AFM results show the formation of granular films with average grain sizes of less than 8nm and with RMS surface roughness of less than 3nm. The most important thing is that these uniformly distributed nanostructures are formed without the use of any surfactant. Thin films are deposited on glass substrate in order to study the optical properties. Band gap values are in the range of 3.65-3.68 eV for SnO₂.

REFERENCES

- Baruah, S. and Dutta, J. (2009), "Effect of seeded substrates on hydrothermally grown ZnO nanorods", *J. Sol-Gel Sci. Technol.*, **50**, 456-464.
- Cetinorgu, E. and Goldsmith, S. (2007), "Chemical and thermal stability of the characteristics of filtered vacuum arc deposited ZnO, SnO₂ and zinc stannate thin films", *J. Phys. D: Appl. Phys.*, **40**, 5220-5226.
- Cun, W., Xinming, W., Jincai, Z., Bixian, M., Guoying, S., Ping'an, P. and Jiamo, F. (2002), "Synthesis, characterization and photocatalytic property of nano-sized Zn₂SnO₄", *J. Mater. Sci.*, **37**, 2989-2996.
- Erslev, P.T., Chiang, H.Q., Hong, D., Wager, J.F. and Cohen J.D. (2008), "Electronic properties of amorphous zinc tin oxide films by junction capacitance methods", *J. Non-Cryst. Solids*, **354**, 2801-2804.
- Horrocks, A.R., Smart, G., Kandola, B. and Price, D. (2012), "Zinc stannate interactions with flame retardants in polyamides; Part 2: Potential synergies with non-halogen-containing flame retardants in polyamide 6 (PA6)", *J. Polym. Degrad. Stab.*, **97**, 645-652.
- Illican, S., Caglar, M. and Caglar, Y. (2010), "Sn doping effects on the electro-optical properties of sol gel derived transparent ZnO films", *J. Appl. Surf. Sci.*, **256**, 7204-7210.
- Kim, K., Annamalai, A., Park, S.H., Kwon, T.H., Pyeon, M.W. and Lee, M. (2012), "Preparation and electrochemical properties of surface-charge-modified Zn₂SnO₄ nanoparticles as anodes for lithium-ion batteries", *Proceeding of '12 J. Electrochimica Acta*. [In Press]
- Li, Z., Zhou, Y., Zhang, J., Tu, W., Liu, Q., Yu, T. and Zou, Z. (2012), "Hexagonal nanoplate-textured micro-octahedron Zn₂SnO₄: Combined effects toward enhanced efficiencies of dye-sensitized solar cell and photoreduction of CO₂ into hydrocarbon fuels", *J. Cryst. Growth Des.*, **12**, 1476-1481.
- Lim, H.N., Nurzulaikh, R., Harrison, I., Lim, S.S., Tan, W.T. and Yeo, M.C. (2011), "Spherical tin oxide, SnO₂ particles fabricated via facile hydrothermal method for detection of mercury (II) ions", *Int. J. Electrochem. Sci.*, **6**, 4329-4340.
- Pal, J. and Chauhan, P. (2009), "Structural and optical characterization of tin dioxide nanoparticles prepared by a surfactant mediated method", *Mat. Charact.*, **60**, 1512-1516.
- Pan, Z.W., Dai, Z.R. and Wang, Z.L. (2001), "Nanobelts of semiconducting oxides", *Sci.*, **291**, 1947-1949.
- Riaz, S., Naseem, S. and Xu, Y.B. (2011), "Room temperature ferromagnetism in sol-gel deposited un-doped ZnO thin films", *J. Sol-Gel Sci. Technol.*, **59**, 584-590.
- Shamala, K.S., Murthy, L.C.S and Narasimha, K. (2004), "Studies on tin oxide films prepared by electron beam evaporation and spray pyrolysis methods", *Bull. Mater. Sci.*, **27**, 295-301.
- Srivastava, A., Rashmi, B. and Jain, K. (2007), "Study on ZnO-doped tin oxide thick film gas sensors", *J. Mater. Chem. Phys.*, **105**, 385-390.
- Tsaroucha, M., Aksu, Y., Irran, E. and Driess, M. (2011), "Synthesis of Stannyl-substituted Zn₄O₄ cubanes as single-source precursors for amorphous tin-doped ZnO and Zn₂SnO₄ nanocrystals and their potential for thin film field effect transistor

- applications”, *J. Chem. Mater.*, **23**, 2428-2438.
- Villarreal, T.L., Boschloo, G. and Hagfeldt, A. (2007), “Nanostructured zinc stannate as semiconductor working electrodes for dye-sensitized solar cells”, *J. Phys. Chem. C*, **111**, 5549-5556.
- Wang, Y., Ramos, I. and Santiago-Avilés, J.J. (2007), “Optical band gap and photoconductance of electrospun tin oxide nanofibers”, *J. Appl. Phys.*, **102**, 093517-1.
- Yadav, B.C., Singh, R., Singh, S. and Dwivedi, K.P. (2012), “Humidity sensing investigations on nanostructured zinc stannate synthesized via chemical precipitation method”, *Int. J. Green Nanotech.*, **4**(1), 37-45.
- Zhang, Y., Guo, M., Zhang, M., Yang, C., Ma, T. and Wang, X. (2007), “Hydrothermal synthesis and characterization of single-crystalline zinc hydroxystannate microcubes”, *J. Cryst. Growth*, **308**, 99-104.